

1 Functional coherence among miRNA targets: a potential metric for assessing biological
2 signal among target prediction methods in non-model species

3

4 Authors:

5

6 Christopher W. Wheat^{1*}

7 Rachel A. Steward¹

8 Yu Okamura^{2,3}

9 Heiko Vogel²

10 Philipp Lehmann^{1,4}

11 Kevin T. Roberts¹

12

13

14

15 ¹Department of Zoology, Stockholm University, Stockholm, Sweden

16 ²Department of Insect Symbiosis, Max Planck Institute for Chemical Ecology, Jena,
17 Germany

18 ³Department of Biological Sciences, Graduate School of Science, University of Tokyo,
19 Tokyo, Japan

20 ⁴Zoological Institute and Museum, Greifswald University, Greifswald, Germany

21

22 * Author for Correspondence: Christopher W. Wheat, Department of Zoology,
23 Stockholm University, Stockholm, Sweden. +46 721 958586.

24 chris.wheat@zoologis.su.se

25

26

27

28 **Abstract**

29

30 Although miRNA regulation of protein production is a likely target of adaptive evolution,
31 high false-positive rates in the identification of mRNAs targeted by miRNAs in non-
32 model species' complicates interpretation of recent advances. Here we document the
33 challenges and then outline steps for the community to address these challenges.

34

35

36

37 **Keywords**

38

39 miRNA, target detection, false-positives, functional coherence, gene set enrichment
40 analysis

41

42

43

44

45 One major revelation of the genomics era is that gene regulatory networks (GRNs)
46 exhibit extensive functional coherence, as most transcription factors regulate the
47 transcription of functionally related modules of genes, resulting in co-expressed genes
48 generally comprising coherent developmental and metabolic pathways (Stuart et al.
49 2003; Wolfe et al. 2005). GRNs are at the core of evolutionary biology studies, since it is
50 the modification of GRNs, as well as their co-option into novel developmental contexts,
51 that is the major axis upon which evolutionary adaptations and novelty arise (Bruce &
52 Patel 2020; Erwin 2021). However, mRNA transcription alone does not determine
53 protein concentrations and hence phenotypes, but rather a diverse set of dynamics,
54 including post-transcriptional and post-translational regulation, significantly modify the
55 transcriptome, forming a key feature of the genotype to phenotype map (Liu et al. 2016;
56 Bartel 2018).

57 Here we focus upon post-transcriptional regulation via microRNAs (miRNAs),
58 ~22 nucleotides (nt) long RNAs. In most animals, miRNAs are produced after
59 transcription via a series of processes (hairpin formation, cleavage, export to cytoplasm,
60 cleavage), then bound by the Argonaute protein, creating a silencing complex that
61 selectively binds mRNA based upon a short (6-8 nt) sequence seed matching between
62 the miRNA and mRNA, primarily in the 3' UTR region of mRNA transcripts, which then
63 initiates various forms of translation repression (Bartel 2018). Via this post-
64 transcriptional action regulating the mRNA to protein production relationship, miRNAs
65 play an important role in developmental progression and physiological functioning
66 (Bartel 2018; Gebert & MacRae 2019). Numerous studies over the past decade, across
67 both invertebrates and vertebrates, have found significant differential expression of
68 miRNA genes associated with adaptive phenotypes, suggesting that these “sculptors” of
69 the transcriptome play an important role in adaptive evolution (Bartel 2018; Leung &
70 Sharp 2010; Fruciano et al. 2021). However, investigating how such differential
71 expression of miRNA causally leads to adaptive phenotypes necessitates identifying the
72 mRNAs that are targeted by miRNAs, as only this allows researchers to make causal
73 connections between differential miRNA expression, protein expression changes, and
74 ultimately differential reproductive success. Unfortunately, identifying which mRNAs are
75 targeted by which miRNAs remains a complex problem (Bracken et al. 2016).

76 Based upon insights from model-species (e.g. humans, flies, worms), animals
77 are expected to have 100's of miRNA families (miRNAs that target the same canonical
78 motif in mRNA), each of which can effectively reduce the protein production of 100's
79 genes. In humans these numbers correspond to about 500 miRNAs, 300 of which can
80 be placed into about 170 gene families, with each family on average
81 posttranscriptionally repressing roughly 400 genes (Bartel 2018). From the perspective
82 of a given mRNA sequence, nearly half of fly (~ 40%) and human (> 60%) mRNAs
83 contain conserved miRNA binding targets, with each mRNA on average containing
84 multiple miRNA binding sites (of the same and/or different miRNA families). Thus,
85 across diverse taxa, miRNAs have the potential to sculpt a large fraction of the
86 transcriptome.

87 Genomic core facilities now routinely provide short RNA sequencing, enabling
88 quantitative assessments of miRNA abundance in nearly any taxa. However, identifying
89 the biologically meaningful targets of differentially expressed miRNA remains
90 challenging, despite technological advances. While direct sequencing of the mRNA pool
91 bound by the silencing complex is possible (crosslinking-immunoprecipitation-
92 sequencing, CLIP-seq), a high concentration of cells is required, with results necessarily
93 averaging over the diverse miRNA regulation dynamics among cells lineages. While a
94 single cell approach has just been developed (Sekar et al. 2023), neither technique is
95 able to identify the miRNAs directly involved.

96 As an initial, or only, foray into miRNA research, many research groups rely upon
97 bioinformatic prediction of miRNA targets in their focal species, for initial interpretation
98 of differential miRNA expression. In animals, miRNA binding to mRNA primarily relies
99 upon 6 to 8 nucleotides of complimentary sequence, referred to as seed pairing. While
100 legions of such short motifs populate the UTR regions of transcriptome, only a small
101 fraction are involved in post-transcriptional repression (Agarwal et al. 2015, 2018;
102 Fridrich et al. 2019). This scenario highlights the inherently challenging nature of target
103 prediction due to the exceptional potential for statistically significant false positives
104 (Fridrich et al. 2019), with the challenge of accurate *in silico* prediction spawning yet
105 another bioinformatics cottage industry (~ 100 different software approaches to date
106 (Fridrich et al. 2019; Kern et al. 2020; Ritchie et al. 2009).

107 Emerging from diverse efforts in model-species to understand miRNA post-
108 transcriptional regulation comes the robust result that signatures of evolutionary
109 conservation, generated due to consistent purifying selection acting over 10 to 100's of
110 millions of years, provides a powerful means of discriminating functionally important
111 seed regions from other candidates in the dynamically evolving UTR regions of mRNA.
112 Indeed, compared to using only identified motifs in a single species, or in combination
113 with various ways of modeling local thermodynamics, only approaches incorporating
114 evolutionary conservation appear accurate (Friedman et al. 2009; Agarwal et al. 2015),
115 though the field continues to explore additional parameters and approaches (Kern et al.
116 2020). Of direct relevance to this journal's readership, the prediction tools most
117 commonly employed by the ecology and evolution, non-model species community are
118 those using data from only one species without information on evolutionary
119 conservation, which exhibit false-positives rates approaching 50% or fail to identify true-
120 positives in well verified experiments (e.g. miRanda, RNAhybrid; (Agarwal et al. 2015;
121 Pinzón et al. 2017; Fridrich et al. 2019; Krüger & Rehmsmeier 2006)).

122 These observations thereby suggest that our community faces extensive
123 challenges, not only when hypothesizing about the potential range of functional impacts
124 of differentially expressed miRNAs, but when trying to conduct functional validation
125 studies. Currently, it is common to see studies intersecting miRNA expression patterns
126 with RNAseq results, scanning for inverse relationships. Unfortunately, finding
127 meaningful negative correlations between miRNA and mRNA levels is likely to
128 challenging, as the power of such correlations depends upon the number of time points
129 in comparison and the accuracy of identified miRNA-mRNA interactions. Given that
130 each miRNA can have hundreds of predicted targets, we fear that without a
131 substantially large dataset of such comparison across tissues and timepoints, such
132 efforts will always be beset by high false-positive rates. In sum, the aforementioned
133 issues highlight the need for an external means of assessing the accuracy of miRNA
134 target set prediction, especially one that could be used by the non-model species
135 community.

136 Here we present rational for an external means of assessing the accuracy of
137 miRNA target set prediction. We take as our starting point that the regulatory network of

138 miRNAs is non-random, as miRNA targets are significantly higher than expected in
139 genes having positive regulatory motifs and being highly-connected GRN components,
140 such as transcription factors (Cui et al. 2006; Bracken et al. 2016). Co-expressed
141 miRNAs, whether co-localized or not, have also been found to target specific genes and
142 pathways (Lee et al. 2012; Xu & Wong 2008; Bracken et al. 2016). Additionally,
143 individual miRNA gene families have been found to exhibit functional coherence in the
144 genes they target (Tsang et al. 2010). Indeed, the functional coherence of mRNA
145 targets is itself central to resolving the paradox between the small post-transcriptional
146 effect of miRNAs upon individual genes and the larger phenotypic effects of miRNAs, as
147 miRNA action upon multiple steps of a pathway is expected to culminate in larger
148 phenotypic impacts (Bracken et al. 2016). However, currently little is known about the
149 extent of such functional coherence across miRNA gene families as a whole. Specially,
150 we can find no global scale analyses of the functional coherence of individual miRNA
151 targets in species other than humans within a disease context (Bracken et al. 2016;
152 Gusev 2008), highlighting the lack of a general understanding of how such coherence
153 varies among taxa. Nevertheless, identifying a signature of functional coherence,
154 beyond informing on the miRNA GRN and how it evolves, could provide a biologically
155 informative metric for assessing *de novo* target predictions in novel taxa.

156 Our work here began with trying to identify the miRNA targets in a novel species,
157 the Green-veined White butterfly *Pieris napi* (Lepidoptera, Pieridae). Ultimately our goal
158 was to identify the miRNAs involved in the different states of diapause progression, but
159 in order to understand patterns of differentially expressed miRNAs, we needed to
160 identify their potential targets in the transcriptome. We present a comparison of different
161 miRNA prediction approaches, finding that only an approach incorporating information
162 on evolutionary constraint results in a detectable functional coherence among the
163 targets per miRNA. In order to validate this finding, we present evidence using miRNA
164 target predictions across model and non-model species that animals generally exhibit
165 extensive functional coherence across miRNA gene families. Therefore, functional
166 coherence provides a biologically informative metric for assessing *de novo* target
167 predictions in novel taxa that could greatly facilitate ability of the ecology and

168 evolutionary genomics community to make logical connections between miRNA to
169 relevant protein expression changes and their eventual phenotypic impacts.

170

171 **Methods**

172 ***Samples, processing, miRNA identification***

173 Data generation, from collection to sequencing through to miRNA gene and seed
174 identification was performed previously (Roberts et al., in review). Although readers are
175 directed to this other work for methodological details (Roberts et al., in review), here
176 they are briefly presented for clarity. A total of 73 samples were taken throughout pupal
177 progression (12 timepoints (0, 3, 6 days direct development; 0,3,6,24,114,144,155 days
178 diapause development), for each of 2 tissues (head, abdomen), each with 3-4 biological
179 replicates). After library construction using Illumina small RNA library kits they were
180 sequenced using HiSeq 2500 50SR, generating an average of 6.9 M reads / library. The
181 miRTrace pipeline was used to check data quality (v1.0.1; (Kang et al. 2018)),
182 contamination and taxonomic bias, followed by filtering and adapter removal (Roberts et
183 al., in review). Using miRDeep2 processing scripts (Friedlander et al. 2011), reads
184 greater than 17bp were mapped against the chromosomal level assembly for *P. napi*
185 genome GCA_905231885.1 (Lohse, Hayward, et al. 2021), with miRNAs detected using
186 *Bombyx mori* and *Heliconius melpomene* as reference miRNA sets.

187

188 ***Target identification***

189 miRNA targets were identified using two separate approaches, the first relying primarily
190 upon evolutionary conservation and the second using data from a single species. Our
191 first approach aligned genomes of 6 species of Pieridae using the software Progressive
192 Cactus (Armstrong et al. 2020), each increasing evolutionary distance from our focal
193 species *P. napi*, which was used as the reference (*P. napi* (GCA_905231885.1; (Lohse,
194 Hayward, et al. 2021), *P. rapae* (GCA_905147795.1; (Lohse, Ebdon, et al. 2021)), *P.*
195 *brassicae* (GCA_905147105.1; (Lohse, Mackintosh, et al. 2021)), *P. macdunnoughii*
196 (Steward et al. 2021). The last two of these 6 genomes were high-quality draft
197 assemblies, using MaSuRCA (Zimin et al. 2017) for genome assembly of Oxford
198 Nanopore Sequencing data and and Illumina short read data for *P. melete*

199 (PRJEB59056, 376 contigs, 320 Mbp, N50 2.6 Mbp, BUSCO: CS:94.1%, CD:4.4%,
200 F:0.3%, M:1.2% (BUSCO v. 5.5.0 (Manni et al. 2021), n:5286, lepidoptera_odb10), and
201 using Flye ver. 2.7 (Kolmogorov et al. 2019) for *Pontia daplidice* (PRJEB59056, 142
202 contigs, 223 Mbp, N50 3.6 Mbp, BUSCO: CS:97.7%, CD:0.5%, F:0.3%, M:1.4%,
203 (n:5286, lepidoptera_odb10). The last common ancestor of these species was
204 approximately 23 million years ago (Chazot et al. 2019). We next sought to identify
205 3'UTR regions that were expressed in the relevant tissue and developmental stage of
206 our miRNA data.

207 Obtaining accurate 3'UTR annotations is challenging for several reasons. First,
208 the 3'UTR per locus is highly variable, with > 65% of human and *Drosophila* loci
209 producing alternative polyadenelated mRNAs across tissues and development (Derti et
210 al. 2012; Ye et al. 2023; Sanfilippo et al. 2017). This gains relevance as the available
211 genomic annotation of our focal species did not use RNAseq data from diapause
212 relevant tissues for their annotation. Second, methods for predicting 3'UTR regions from
213 DNA alone, or even with RNAseq data, perform with high variability across species and
214 in general, poorly in non-model species (Ye et al. 2023; Bryce-Smith et al. 2023), and
215 though some have tried to directly address this (Huang & Teeling 2017), obtaining
216 meaningful UTR predictions is challenging in novel species. Thus, in order to efficiently
217 move beyond data and bioinformatic limitations, here we deployed a simplified
218 approach for exploring potential 3'UTR regions for our focal species.

219 We assessed the 3'UTR annotation for the *P. napi* genome and found that it had
220 overpredicted UTR regions (GCA_905231885.1; (Lohse, Hayward, et al. 2021), such
221 that UTR regions routinely overlapped with flanking genes. In addition, at the time of our
222 analyses, the annotation of GCA_905231885.1 available from the Darwin Tree of Life
223 Program relied on an early annotation pipeline that was not optimized for Lepidoptera.
224 Accordingly, we chose to rely upon a *de novo* genome annotation we previously
225 generated (Steward et al., in review). This *de novo* annotation was produced using the
226 BRAKER2 pipeline (v.2.1.5, (Brůna et al. 2020; Hoff et al. 2016; Ter-Hovhannisyan et
227 al. 2008; Stanke et al. 2006, 2008; Lomsadze et al. 2005; Hoff et al. 2019), run in
228 protein mode using Arthropoda OrthoDB (v.10) reference proteins. This annotation
229 contained 123,638 exons, 16,449 genes and was found to contain 98.4% complete

230 BUSCOs for Lepidoptera_ODB10. Comparisons between this annotation and two
231 accessed from the Darwin Tree of Life revealed the BRAKER2 annotation to be the
232 most complete (i.e. fewest fragmented BUSCOs, a small proportion of single exon
233 genes, and more total estimated transcripts (see Supplementary methods; Table S1, S2
234 in Steward et al., in review).

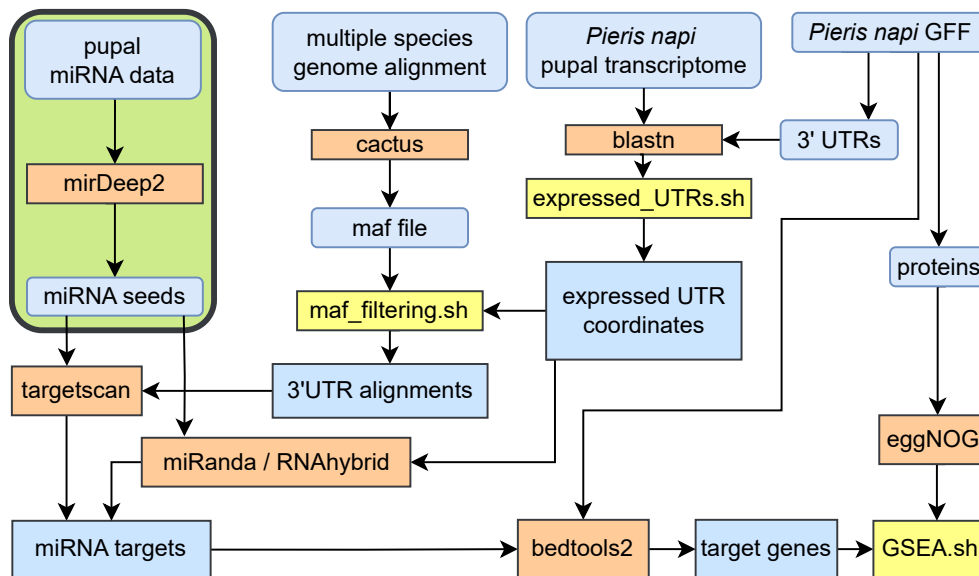
235 Among moths and flies, the majority of 3'UTR regions are expected to be within 1
236 kb of the stop codon in the terminal coding exon, based upon detailed studies from
237 several *Drosophila* species (Sanfilippo et al. 2017; Wang et al. 2019) and 3'UTR lengths
238 for the an exemplar moth (*Bombyx mori* mean=923 bp, n=27,556) and butterfly
239 (*Heliconius melpomene* mean=600, n=11,770) downloaded from UTRdatabase
240 (Lo Giudice et al. 2023). While alternative UTRs in animals can involve spliced introns,
241 the frequency in 3'UTR regions are lower than 5'UTR, and usually < 10% (Mignone et
242 al. 2002). Based upon these expectations of 3'UTRs, we generated a bed file of likely
243 3'UTR regions, extending 1kb beyond every stop codon (and containing 9 codons (27
244 bp) prior to the terminal codon), of every protein isoform. We then assessed whether
245 any of these candidate 3'UTR regions had a significant match via blastn when searched
246 against the assembled transcriptome of an RNAseq dataset. The assembled
247 transcriptome was generated using Trinity (Haas et al. 2013), default parameters, with
248 RNAseq data comprising all of the same tissues and timepoints of our miRNA samples
249 (Pruisscher et al. 2021). Alignments were filtered to only include candidate 3'UTR
250 regions that had at least 70 bp of 3pUTR (filter settings: DNA identity > 90%, e-value <
251 0.000001, bitscore > 300, alignment length > 100 bp; NCBI BLAST v. 2.2.28+;
252 (Camacho et al. 2009). Coordinates for these post-filtered 3'UTR regions, which we
253 expect to be expressed 3'UTRs, were then used to identify these regions in the *P. napi*
254 genome, then whole genome alignment of all species, followed by the extraction of each
255 expressed 3'UTR region, which were then used as the input for conserved miRNA
256 target identification via targetscan_70.pl, part of TargetScan v.7 (Agarwal et al. 2018).
257 Manipulation of GFF files used bedtools2 (Quinlan & Hall 2010), which was also used to
258 assign nearest coding gene ID to each candidate 3'UTR region, while alignment filtering
259 used maffilter, with default settings unless indicated (remove_duplicates=yes,
260 reference=Pnapi, min_size=6), min_length=50, dist_max=1200; (Dutheil et al. 2014).

261 The other input file for targetscan_70.pl was the seed sequences for each of the
 262 identified miRNA genes, predicted from mirDeep2 (Roberts et al., in review).

263 For each identified target region, the resulting output provides information on
 264 species depth and seed size, which can be used to filter for differing degrees of
 265 evolutionary conservation. Species depth indicates the number of species having the
 266 identical target sequence in the alignment, ranging from all of the species down to only
 267 2 species. Targets only found in 2 of the 6 species likely identify a region of lower
 268 evolutionary constraint compared to targets identical across all species. Seed size of
 269 the identified target can vary in size from an 8-mer down to a 6-mer, indicating the
 270 length of base pairs of the identified target. Targets shorter in length are more likely to
 271 occur by random chance compared to those of longer length. We use this information to
 272 explore the quality of targets in later analyses.

273 Our second approach for miRNA target prediction used only two files as the input
 274 for miRanda (Enright et al. 2003) and RNAhybrid (Krüger & Rehmsmeier 2006). These
 275 were the expressed 3'UTR coordinates for *P. napi* and seed sequences for *P. napi*, both
 276 of which were described above. Both programs were run on default settings. Thresholds
 277 for targets were set at e-value < 0.1 for miRanda, and p-value < 0.1 for RNAhybrid.

278



279

280 Fig. 1. Flowchart of miRNA target detection in *Pieris napi*, using two methods that lead
 281 to gene set enrichment analyses (GSEA). Shown are the data files (blue), various

282 software programs (orange), and custom bioinformatic scripts (yellow) that were used.
283 Generation of miRNA data through to miRNA seed input file is from previously
284 published work (green enclosed portion of flow chart; Roberts et al., in review). Made
285 using diagrams.net.

286

287

288 ***Functional coherence via gene set enrichment analysis***

289 Target sets predicted per miRNA family were assessed for their functional coherence
290 via gene set enrichment analysis (GSEA) using the R package topGO v2.46 (Alexa &
291 Rahnenfuhrer 2023), with inputs of GO terms assigned to the coding regions of genes
292 having identified 3'UTR targets. For each GSEA of a miRNA target set, we took the -
293 log₁₀ P-values of the top ten most significant categories, and quantified their distribution
294 as a function of the number of aligned species having identical seed sequences, and for
295 different seed pairing lengths, from 6mer to 8mer.

296

297 ***Comparative assessment of functional coherence***

298 In order to gain a robust assessment of miRNA functional coherence, with miRNA target
299 sets independent of our work and for model species having higher quality target
300 prediction, we repeated our analyses on the miRNA targets from 4 additional diverse
301 animals. Three datasets were downloaded from TargetScan databases (*Homo sapiens*:
302 TargetScanHuman release 8.0, Predicted_Targets_Info.default_predictions.txt
303 (McGeary et al. 2019); *Mus musculus*: TargetScanMouse release 8.0,
304 Predicted_Targets_Info.default_predictions.txt (McGeary et al. 2019); *Drosophila*
305 *melanogaster*: TargetScanFly release 7.2,
306 Predicted_Targets_Info.default_predictions.txt, (Agarwal et al. 2018)), while predicted
307 cichlid targets for *Oreochromis niloticus* (Mehta et al. 2022), were provided by Dr. T.
308 Mehta upon request. Note that for each TargetScan species dataset, in order to connect
309 miRNA ID to coding gene ID to GO terms of the latter, for the relevant genome
310 assembly, its GFF annotation was downloaded and protein sequences per ID extracted
311 using gffread from cufflinks-2.2.1 (Trapnell et al. 2010), for which GO annotations were
312 generated using functional annotation via orthology assignment, implemented in the

313 online server eggNOG using default settings (Huerta-Cepas et al. 2019), which was
314 then joined to the miRNA table downloaded from the relevant TargetScan database. An
315 estimate of the evolutionary depth over which 3'UTR alignments were made in order to
316 assess evolutionary constrain was estimated from. Ages for each clades of data upon
317 which miRNA targets were based, i.e. the age of the relevant crown groups (the
318 paraphyletic *Drosophila* genus at 53 MYA (Suvorov et al. 2022); the dataset for *H.*
319 *sapiens* involved using 84 of 100 species of the UCSC multiz alignment (Agarwal et al.
320 2015), including all species sister to, *Latimeria chalumnae*, as well as this coelacanth,
321 with their crown age estimated at roughly 400 MYA (Amemiya et al. 2013); the dataset
322 for *M. musculus* only included 52 species of the 60-way multiz alignment of UCSC, and
323 has a similar crown age as *H. sapiens*; the dataset for target *O. niloticus* has a crown
324 age estimated at 10 MYA (Mehta et al. 2022).

325

326 **Results and Discussion**

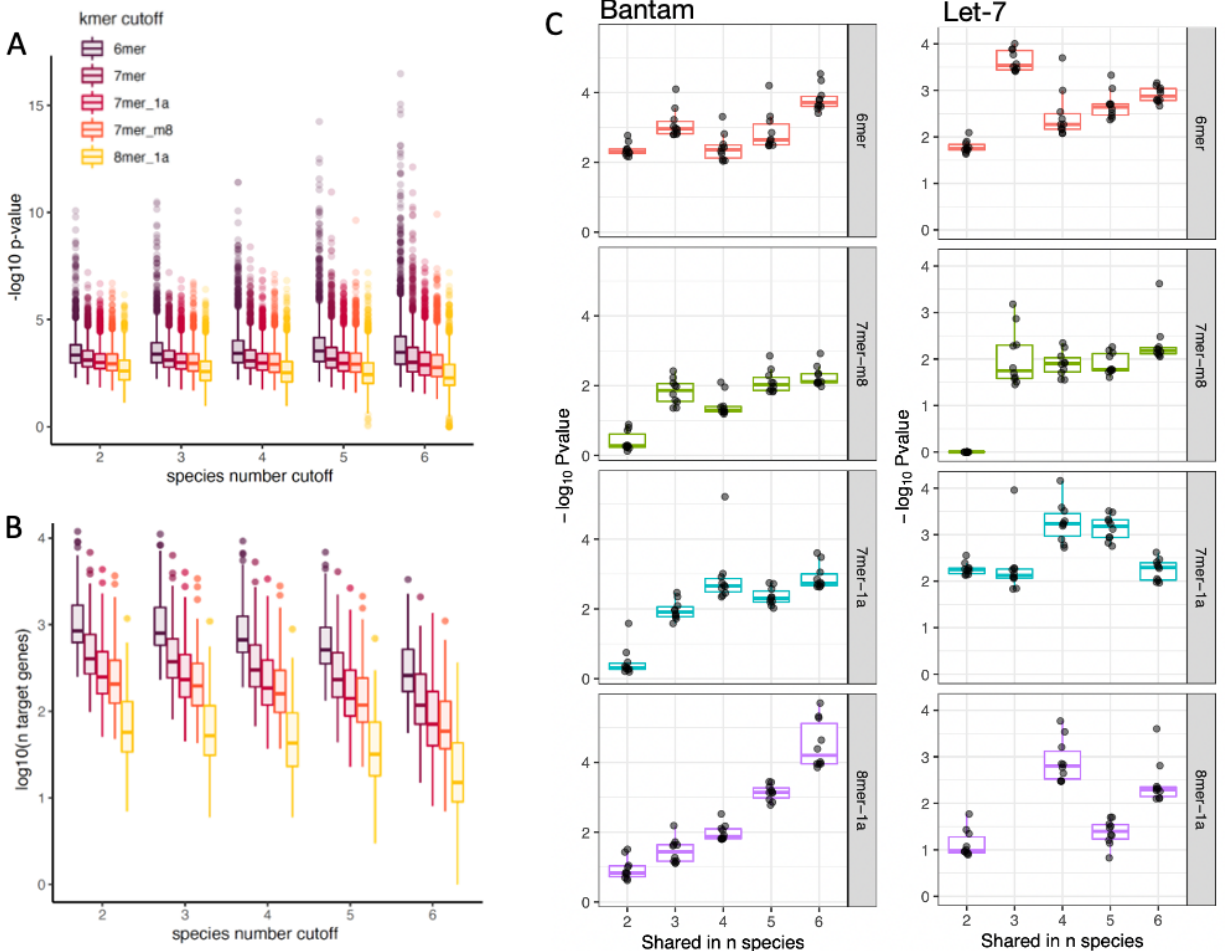
327 An extensive miRNA sequencing effort has recently identified 257 miRNAs expressed
328 during pupal development of *P. napi* (236 expressed in head tissue, 207 in the
329 abdomen; Roberts et al., in review). Here we use this data to predict mRNA targets of
330 these miRNAs in *P. napi*. We began by identifying which mRNAs, among all candidate
331 3'UTR regions in the genome of *P. napi*, were expressed in a tissue matched RNAseq
332 transcriptome assembly. We then identified these 3'UTR regions if mRNA in a
333 multispecies, whole-genome alignment (n=6 species of Pieridae, Lepidoptera) that span
334 nearly 23 million years of divergence (Chazot et al. 2019). The resulting 3'UTR
335 alignment, together with the seed sequences from the identified miRNA genes of *P.*
336 *napi*, were then used as input for TargetScan v.7, which uses evolutionary conservation
337 in 3'UTRs to predict miRNA targets (Agarwal et al. 2018).

338 Next, we sought an independent means of quantifying whether these predicted
339 target sets per miRNA gene had more biological meaning than random sets, as
340 critiques of target prediction methods suggest that target sets generate from tools such
341 as miRAanda and RNAhybrid may be dominated by false positives (Fridrich et al. 2019;
342 Pinzón et al. 2017; Krüger & Rehmsmeier 2006). We reasoned that since a general
343 feature of gene regulatory networks (GRN) is their extensive functional coherence of

344 regulated genes, as most transcription factors regulate related modules of genes (Stuart
345 et al. 2003; Wolfe et al. 2005), the same is likely true for the targets of miRNA (see
346 Methods for additional discussion). Functional coherence was quantified using gene set
347 enrichment analysis (GSEA) upon the predicted set of gene targets for each miRNA,
348 using the average significance of the top ten most enriched GO categories as the
349 representative metric.

350 In order to assess whether there was any functional coherence in our predicted
351 targets, we quantified GSEA of the miRNA target sets using variable levels of
352 evolutionary constraint. TargetScan output provides two axes upon which to vary
353 evolutionary constraint in miRNA target prediction. First, we used differing thresholds of
354 constraint upon the species alignment of the 3'UTR, by varying the number of species
355 for which the seed site was required to be identical. Our lowest evolutionary constraint
356 level required only 2 species to have identical sequences in the alignment for the
357 miRNA seed site (the lowest threshold we could set), while our most stringent required
358 all 6 species to have the same identical sequence for the seed site. Second, there are 5
359 different sizes of target sites for the seed match region of the 3'UTR, ranging from 6 bp
360 (6mer) to 8 bp (8mer) in length. Requiring target sites to be longer in length is a more
361 stringent requirement. In combination, our most relaxed setting was 6mer for only 2
362 species in the alignment, while our most constrained was 8mer for all species. In order
363 to assess the relative tradeoff across these axes of constraint in the prediction of
364 miRNA targets, we explored our results extensively (fig. 2 A,B). As the stringency
365 increases, via increasing the number of species having target seed or increasing the
366 size of the seed match category, the predicted number of targets per miRNA gene
367 decreases, suggesting there is a biological signal in our target prediction method. While
368 these results are highly variable across miRNA genes (fig. 2C), we concluded that a
369 good balance between over-prediction and power was using a 7mer seed match size
370 and higher (termed 7mer-inclusive, which includes all targets from 7mer variants and
371 8mer) that is present and conserved across all of the aligned species.

372



373

374 Fig. 2. Assessment of GSEA results across predicted targets per miRNA gene. (A)
 375 Significance of the top 10 GO terms per target set per miRNA gene (each dot is one
 376 term) shown as a boxplot of all results, as a function of the number of species for which
 377 seed was identical, for each of 5 different sizes of site type of the seed match (color
 378 scale purple to yellow). As the stringency of predicted targets increases from being
 379 found only in 2 species to all 6 species, the significance values increase for the smaller
 380 seed match sizes (e.g. 6mers increase while 8mers do not). (B) Number of targets per
 381 miRNA gene (each dot is count for a miRNA gene), across different prediction
 382 thresholds of species number and miRNA seed match size (as in A). As the stringency
 383 increases, via increasing the number of species having target seed or increasing the
 384 size of the seed match category (color scale purple to yellow), the predicted number of
 385 targets per miRNA gene decreases (6mer in 2 species is largest set, 8mer in 6 species
 386 is the smallest). (C) Shown are GSEA results for two miRNA genes (left is Bantam, right

387 is Let-7), displaying effects of stringency increase on significance of the top 10 GO
388 terms per target set per miRNA gene. These exemplify the range of variation between
389 miRNA genes in their GSEA results, with Bantam exhibiting a strong increase in GSEA
390 P-value as evolutionary constraint is maximized (8mer-1a panel) and Let-7 lacking this
391 trend.

392

393

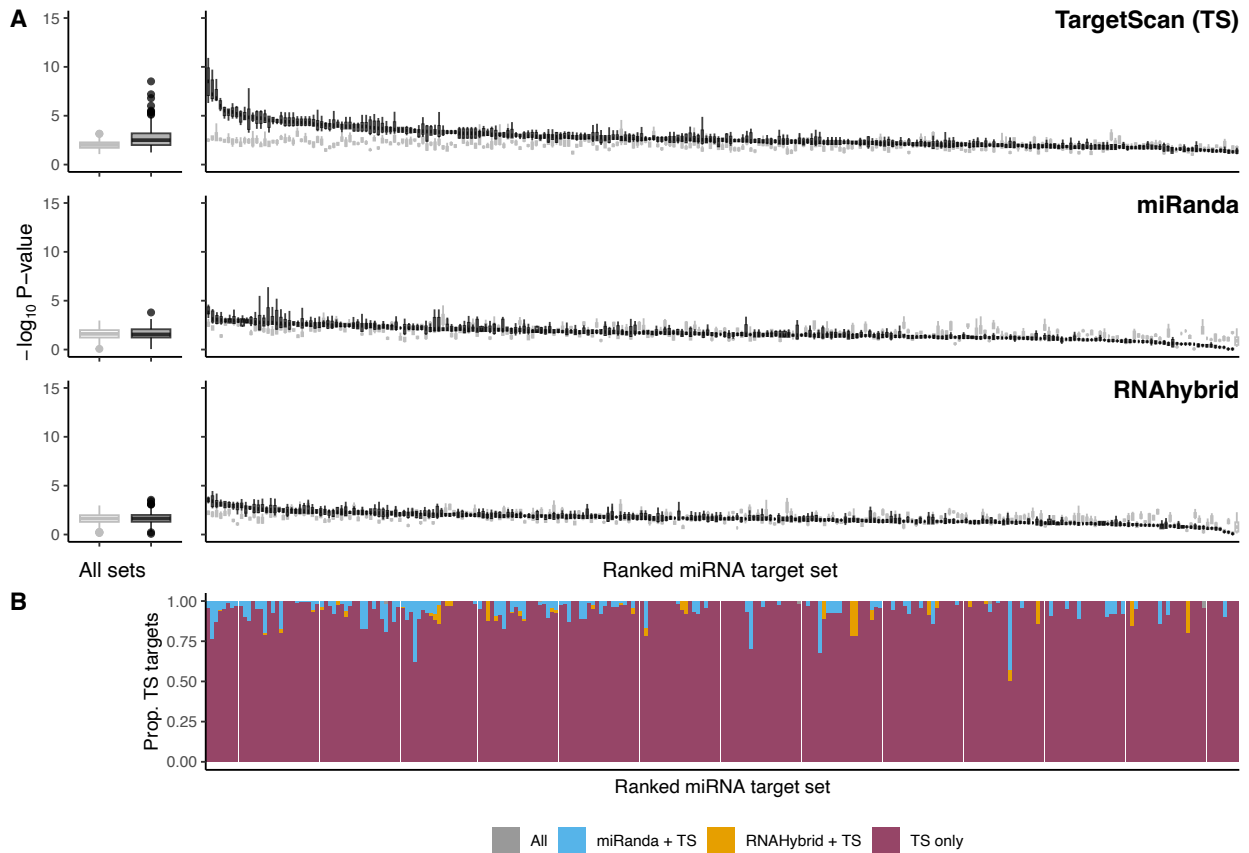
394 For comparison, we also used single species target prediction methods. Using
395 the 3'UTR regions of *P. napi* and seed sequences of miRNA genes as input, we used
396 the most commonly employed target prediction tool by the ecological and evolutionary
397 genomics community, miRanda (Enright et al. 2003). We additionally employed a
398 second single species tool with the same input data, RNAhybrid (Krüger & Rehmsmeier
399 2006). In order to compare the predicted targets across these tools, we quantified their
400 relative functional coherence via GSEA using the 7mer-inclusive conservation threshold
401 (described above). As a control, a GSEA was conducted on random sets of gene
402 targets conditional on the set size of the observed miRNA targets, which we used as our
403 background expectation of significance given concerns about GSEA significance
404 thresholds when working with miRNA targets (Bleazard et al. 2015).

405 The predicted targets of each miRNA from both methods exhibited significant
406 GSEA results, with average P-values for miRanda of 0.0185 and 0.0420 for RNAhybrid
407 (fig. 3a). However, GSEA results on sets of randomly drawn genes had P-value
408 distributions that entirely overlapped with the gene set targets predicted by these
409 methods (fig. 3a). Thus, GSEA P-value for targets from miRanda, RNAhybrid, and
410 random draws were lower than nominal P-value significance thresholds (i.e., $\alpha =$
411 0.05), highlighting two issues. First, these results exemplify previously noted challenges
412 of GSEA when investigating miRNA targets (Bleazard et al. 2015), in that resulting P-
413 values are poorly controlling for diverse many to many relationships, as GSEA were not
414 designed for such relationships. Second, neither miRanda nor RNAhybrid predicted
415 targets that performed better than random.

416 In stark contrast to the previous results, miRNA targets predicted using
417 evolutionary conservation via TargetScan exhibited extensive functional coherence (fig.

418 3a), with GSEA P-values much higher than random draws. This result suggests two
419 mutually exclusive explanations. Either *P. napi* has miRNA targets that lack functional
420 coherence, which could explain the miRanda and RNAhybrid results and therefore
421 justify continued use of such tools by the non-model species community, or the miRNAs
422 of this butterfly exhibit functional coherence and only biologically meaningful target sets
423 can reveal this pattern. When facing variable results among target prediction methods,
424 studies in the non-model species community commonly intersect results from various
425 target prediction methods, despite this being explicitly discouraged by experts in the
426 miRNA field (Fridrich et al. 2019; Ritchie et al. 2009). To quantify the performance of
427 such an intersection approach, here we assess the overlap of targets from miRanda
428 and RNAhybrid with respect to target predictions from TargetScan. We find no
429 substantial overlap across these three methods. Further, the level of overlap among
430 methods does not covary with the degree of functional coherence observed in our
431 TargetScan results (fig. 3b).

432



434

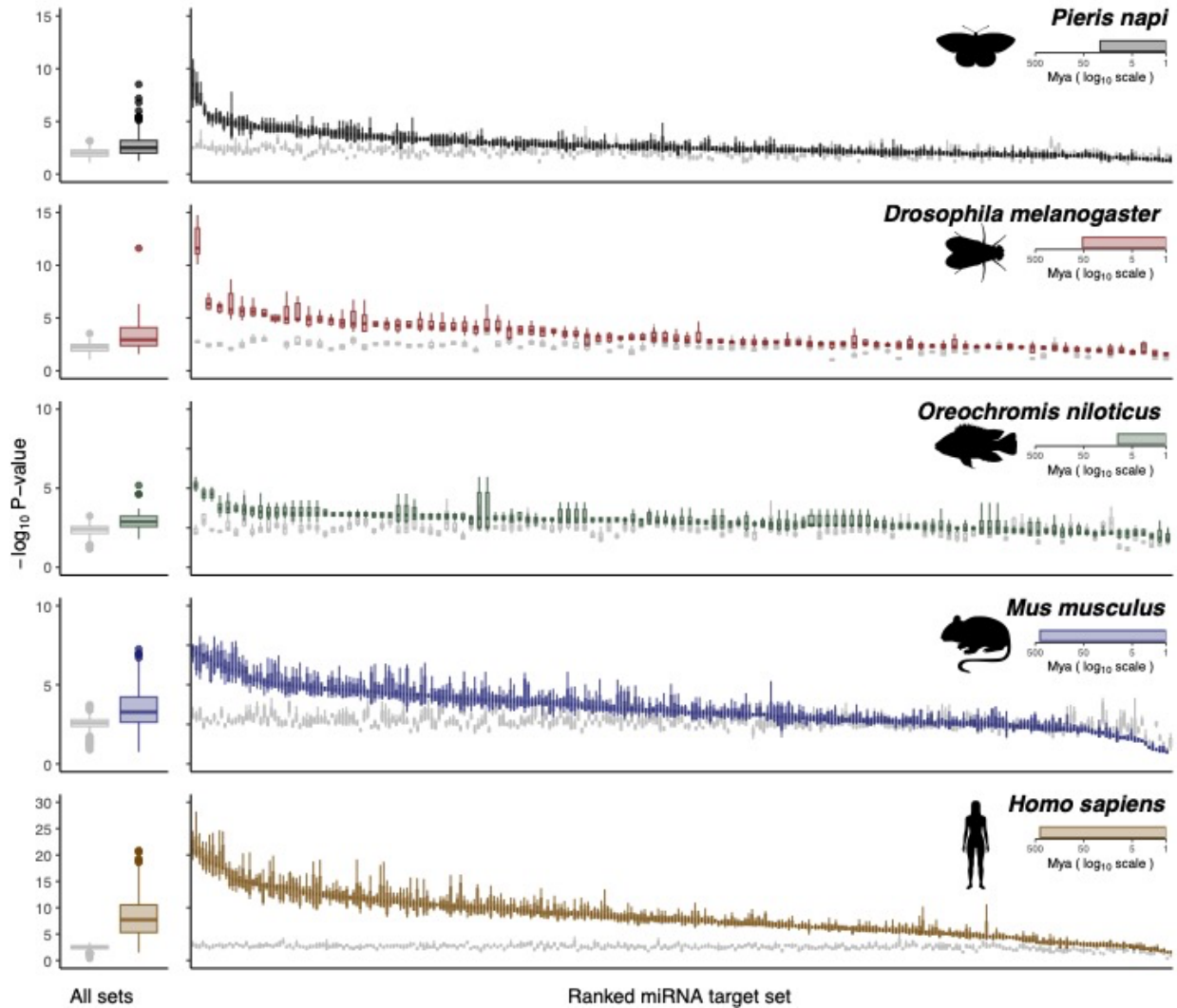
435 Fig. 3. The functional coherence of miRNA targets across animals measured using
 436 gene set enrichment analysis (GSEA). (A) Comparison of the functional coherence of
 437 miRNA target predictions and their relationships, predicted in the butterfly *Pieris napi*.
 438 Gene set enrichment analysis P-values for top 10 GO terms for each miRNA (Y-axis) for
 439 targets predicted using Targetscan (top panel), miRanda (middle panel), RNAhybrid
 440 (lower panel). Left-hand panels summarize median P-values for random (light grey) and
 441 predicted (black) miRNA target sets, while right-hand panels show results each miRNA
 442 target set. (B) Intersection of predicted targets from all three methods in relation to
 443 TargetScan results, shown as a proportion. Order of miRNAs along X axis are by mean
 444 P-value based upon Targetscan GSEA results.

445

446

447 In order to discriminate between the two aforementioned explanations, we next
 448 quantified functional coherence using four published miRNA target sets. Across diverse

449 metazoans, from arthropods to vertebrates, we found extensive functional coherence
450 across many miRNAs (fig. 4). In each species, a large fraction of predicted miRNAs
451 exhibited a significantly greater functional coherence than background. Importantly, all
452 of these previously published target sets were generated using the TargetScan
453 framework, using phylogenetic conservatism of miRNA binding sites as a core
454 identification criteria (Friedman et al. 2009; Agarwal et al. 2015). Common to all species
455 is a substantial variation among miRNA gene sets in their functional coherence (the left
456 vs right side of the P-value ranked distribution of miRNA genes). Whether this variation
457 arises due to unequal coherence across miRNAs, variation in the functional annotation
458 of relevant targets, poorly annotated 3'UTRs, or other factors warrants attention.
459 However, the extensive functional coherence seen across nearly all miRNA genes in *H.*
460 *sapiens* suggests such variation likely arises due to factors other than unequal
461 coherence among the target sets of miRNA genes. Among these diverse metazoans,
462 the lower functional coherence observed in these cichlids likely arises due to the young
463 age of the clade analyzed (~ 10 million years), as this necessarily results in a lower
464 power via phylogenetic conservatism. Highlighting the need and challenges of
465 bioinformatic target assessment in young clades, this clade of cichlids is an exemplar of
466 adaptive radiations, having generated > 2000 species in the 10 million years, making
467 observations of their massive reorganization of the miRNA GRN incredibly intriguing for
468 evolutionary study (Mehta et al. 2022).
469
470



471
 472
 473
 474
 475
 476
 477
 478
 479
 480
 481
 482
 483

Fig. 4. Functional coherence of miRNA targets across animals measured using gene set enrichment analysis (GSEA). Left-hand boxplots summarize median P-values for random and predicted miRNA target sets, while right-hand boxplots show P-values for the top 10 enriched GO terms per per miRNA gene, ordered by median GSEA P-value within each species. Results from predicted targets are colored while results from randomly selected genes are shown in gray. Inset horizontal bars indicate crown age (million years) of the species used to generate miRNA target predictions. Results from *P. napi* (fig. 3a) are presented here, allowing for direct comparison with four divergent taxa whose published datasets were generated using TargetScan.

484 **Conclusions**

485 Functional coherence in the targets of miRNA genes appears to be common in
486 the tree of life. Using this observation, together with an in-depth study of miRNA targets
487 in a non-model species, our finding of no biological signal among the miRNA targets
488 produced by miRanda and RNAhybrid predictions is consistent with previous findings
489 and warnings of their low precision (Fridrich et al. 2019; Agarwal et al. 2015, 2018;
490 Pinzón et al. 2017; Ritchie et al. 2009). We conclude that a substantial body of research
491 may benefit from revising hypotheses based upon miRNA expression patterns, when
492 those hypotheses relied upon miRNA target prediction lacking measures of evolutionary
493 conservation.

494 Much remains to be discovered about the role the miRNAs play in adaptive
495 evolution and there has never better time for investigating the role of miRNA
496 posttranslational repression in novel species. An ever-increasing diversity of high-quality
497 genomes provides an unprecedented opportunity for exploiting evolutionary
498 conservation via recent advances in miRNA target prediction (Agarwal et al. 2018). We
499 note however that target predictions are merely another set of hypotheses. Since most
500 miRNAseq studies are also coupled with RNAseq, we further note that correlations
501 between increased miRNA expression and decreases in putative mRNA target
502 expression are also hypotheses fraught with a potential for high false-positives, given
503 the diverse patterns of expression in such datasets coupled with generally few sets of
504 diverse sampling points. Finally, while identified miRNA function in model species can
505 certainly aid hypothesis formulation of miRNA impacts, such relies upon increasingly
506 tenuous assumptions of evolutionarily conserved function (Rusin 2023).

507 Perhaps the most important way forward for the non-model species community
508 seeking to connect miRNA expression changes with adaptive phenotypes will be via
509 harnessing of emerging gene manipulation technologies in the testing of functional
510 hypotheses (Gudmunds et al. 2022). While the diverse many-to-many relationships
511 inherent in the miRNA GRN necessitate careful design and interpretation of such
512 experiments (Bartel 2018), these also offer unique opportunities. For example, consider
513 a scenario where many independent miRNA genes target the same seed sequence
514 within mRNA. While KO of all such miRNA genes could be lethal, knock out of one,

515 several, or many genes within such a gene family could effectively titrate phenotypic
516 effects. Additionally, advances in single cell sequencing of RNA could greatly advance
517 insights (Sekar et al. 2023), especially in the assessment of miRNA interactions with
518 mRNA GRNs across diverse tissues and developmental courses.

519 In conclusion, numerous studies across diverse taxa document differential
520 expression of miRNAs suggestive of a potentially important role in adaptive evolutionary
521 phenotypes. However, much work remains to be conducted in order to establish such
522 genotype to phenotype connections. Here, by drawing attention to the challenges of *de*
523 *novo* miRNA target prediction, we hope that more biologically meaningful hypotheses
524 will emerge that can then be tested by modification of miRNA genes or their target sites,
525 much as mRNA based hypotheses are now routinely explored via CRE and coding
526 region manipulations (Gudmunds et al. 2022).

527

528 **Acknowledgements**

529 This work greatly benefited from discussion with Marc Frilander, Emilio Sanchez, and
530 members of the Wheatlab. We also thank the Society for Molecular Biology and
531 Evolution for allowing C.W.W. to present this work at, and receive extensive feedback
532 from attendees, at the SMBE annual meeting in 2023. This work was supported by the
533 Carl Tryggers Stiftelse (grant no. CTS20-242), the Swedish Research Council (2015-
534 04218, 2017-04386, 2019-03441), and the Knut and Alice Wallenberg Foundation
535 (grant number 2012.0058).

536

537 **Author contributions**

538 C.W.W. performed all the bioinformatic analyses involved in the generation of miRNA
539 targets using TargetScan. R.S. provided R code for generating systematic GSEA for all
540 miRNA gene families and plotting the results. P.E. and K.R. ran the miRanda and
541 RNAhybrid analyses. C.W.W. and K.R. conceived of the study, with input from R.S.
542 C.W.W. wrote the manuscript with feedback from K.R. and the other coauthors. Y.O.
543 and H.V. provided two genomes for analyses. All authors approve of the manuscript.

544

545 **Data Availability Statement**

546 Scripts will be made available upon submission for review and publication.

547

548 **References**

549 Agarwal V, Bell GW, Nam J-W, Bartel DP. 2015. Predicting effective microRNA target sites in
550 mammalian mRNAs Izaurrealde, E, editor. eLife. 4:e05005. doi: 10.7554/eLife.05005.

551 Agarwal V, Subtelny AO, Thiru P, Ulitsky I, Bartel DP. 2018. Predicting microRNA targeting
552 efficacy in Drosophila. Genome Biol. 19:152. doi: 10.1186/s13059-018-1504-3.

553 Alexa A, Rahnenfuhrer J. 2023. topGO: Enrichment Analysis for Gene Ontology. doi:
554 10.18129/B9.bioc.topGO.

555 Amemiya CT et al. 2013. The African coelacanth genome provides insights into tetrapod
556 evolution. Nature. 496:311–316. doi: 10.1038/nature12027.

557 Armstrong J et al. 2020. Progressive Cactus is a multiple-genome aligner for the thousand-
558 genome era. Nature. 587:246–251. doi: 10.1038/s41586-020-2871-y.

559 Bartel DP. 2018. Metazoan MicroRNAs. Cell. 173:20–51. doi: 10.1016/j.cell.2018.03.006.

560 Bleazard T, Lamb JA, Griffiths-Jones S. 2015. Bias in microRNA functional enrichment analysis.
561 Bioinformatics. 31:1592–1598. doi: 10.1093/bioinformatics/btv023.

562 Bracken CP, Scott HS, Goodall GJ. 2016. A network-biology perspective of microRNA function
563 and dysfunction in cancer. Nat. Rev. Genet. 17:719–732. doi: 10.1038/nrg.2016.134.

564 Bruce HS, Patel NH. 2020. Knockout of crustacean leg patterning genes suggests that insect
565 wings and body walls evolved from ancient leg segments. Nat. Ecol. Evol. 4:1703–1712.
566 doi: 10.1038/s41559-020-01349-0.

567 Brůna T, Hoff KJ, Lomsadze A, Stanke M, Borodovsky M. 2020. BRAKER2: Automatic
568 Eukaryotic Genome Annotation with GeneMark-EP+ and AUGUSTUS Supported by a
569 Protein Database. bioRxiv. 2020.08.10.245134. doi: 10.1101/2020.08.10.245134.

570 Bryce-Smith S et al. 2023. *Extensible benchmarking of methods that identify and quantify*
571 *polyadenylation sites from RNA-seq data*. Bioinformatics doi:
572 10.1101/2023.06.23.546284.

573 Camacho C et al. 2009. BLAST+: architecture and applications. BMC Bioinformatics. 10:421.
574 doi: 10.1186/1471-2105-10-421.

575 Chazot N et al. 2019. Priors and Posteriors in Bayesian Timing of Divergence Analyses: The
576 Age of Butterflies Revisited. Syst. Biol. 68:797–813. doi: 10.1093/sysbio/syz002.

577 Cui Q, Yu Z, Purisima EO, Wang E. 2006. Principles of microRNA regulation of a human cellular
578 signaling network. Mol. Syst. Biol. 2:46. doi: 10.1038/msb4100089.

579 Derti A et al. 2012. A quantitative atlas of polyadenylation in five mammals. Genome Res.
580 22:1173–1183. doi: 10.1101/gr.132563.111.

581 Dutheil JY, Gaillard S, Stukenbrock EH. 2014. MafFilter: a highly flexible and extensible multiple
582 genome alignment files processor. BMC Genomics. 15:np. doi: 10.1186/1471-2164-15-
583 53.

584 Enright AJ et al. 2003. MicroRNA targets in Drosophila. Genome Biol. 5:R1. doi: 10.1186/gb-
585 2003-5-1-r1.

586 Erwin DH. 2021. A conceptual framework of evolutionary novelty and innovation. Biol. Rev.
587 96:1–15. doi: <https://doi.org/10.1111/brv.12643>.

588 Fridrich A, Hazan Y, Moran Y. 2019. Too Many False Targets for MicroRNAs: Challenges and
589 Pitfalls in Prediction of miRNA Targets and Their Gene Ontology in Model and Non-
590 model Organisms. *BioEssays*. 41:1800169. doi: 10.1002/bies.201800169.

591 Friedlander MR, Mackowiak SD, Li N, Chen W, Rajewsky N. 2011. miRDeep2 accurately
592 identifies known and hundreds of novel microRNA genes in seven animal clades.
593 *Nucleic Acids Res.* 40:37–52. doi: 10.1093/nar/gkr688.

594 Friedman RC, Farh KK-H, Burge CB, Bartel DP. 2009. Most mammalian mRNAs are conserved
595 targets of microRNAs. *Genome Res.* 19:92–105. doi: 10.1101/gr.082701.108.

596 Fruciano C, Franchini P, Jones JC. 2021. Capturing the rapidly evolving study of adaptation. *J.*
597 *Evol. Biol.* 34:856–865. doi: 10.1111/jeb.13871.

598 Gudmunds E, Wheat CW, Khila A, Husby A. 2022. Functional genomic tools for emerging
599 model species. *Trends Ecol. Evol.* 37:1104–1115. doi: 10.1016/j.tree.2022.07.004.

600 Gusev Y. 2008. Computational methods for analysis of cellular functions and pathways
601 collectively targeted by differentially expressed microRNA. *Methods*. 44:61–72. doi:
602 10.1016/j.ymeth.2007.10.005.

603 Haas BJ et al. 2013. De novo transcript sequence reconstruction from RNA-seq using the Trinity
604 platform for reference generation and analysis. *Nat. Protoc.* 8:1494–1512. doi:
605 10.1038/nprot.2013.084.

606 Hoff KJ, Lange S, Lomsadze A, Borodovsky M, Stanke M. 2016. BRAKER1: Unsupervised
607 RNA-Seq-Based Genome Annotation with GeneMark-ET and AUGUSTUS: Table 1.
608 *Bioinformatics*. 32:767–769. doi: 10.1093/bioinformatics/btv661.

609 Hoff KJ, Lomsadze A, Borodovsky M, Stanke M. 2019. Whole-Genome Annotation with
610 BRAKER. In: *Gene Prediction: Methods and Protocols*. Kollmar, M, editor. *Methods in*
611 *Molecular Biology* Springer: New York, NY pp. 65–95. doi: 10.1007/978-1-4939-9173-
612 0_5.

613 Huang Z, Teeling EC. 2017. ExUTR: a novel pipeline for large-scale prediction of 3'-UTR
614 sequences from NGS data. *BMC Genomics*. 18:847. doi: 10.1186/s12864-017-4241-1.

615 Huerta-Cepas J et al. 2019. eggNOG 5.0: a hierarchical, functionally and phylogenetically
616 annotated orthology resource based on 5090 organisms and 2502 viruses. *Nucleic Acids*
617 *Res.* 47:D309–D314. doi: 10.1093/nar/gky1085.

618 Kang W et al. 2018. miRTrace reveals the organismal origins of microRNA sequencing data.
619 *Genome Biol.* 19:213. doi: 10.1186/s13059-018-1588-9.

620 Kern F et al. 2020. What's the target: understanding two decades of in silico microRNA-target
621 prediction. *Brief. Bioinform.* 21:1999–2010. doi: 10.1093/bib/bbz111.

622 Kolmogorov M, Yuan J, Lin Y, Pevzner PA. 2019. Assembly of long, error-prone reads using
623 repeat graphs. *Nat. Biotechnol.* 37:540–546. doi: 10.1038/s41587-019-0072-8.

624 Krüger J, Rehmsmeier M. 2006. RNAhybrid: microRNA target prediction easy, fast and flexible.
625 *Nucleic Acids Res.* 34:W451–W454. doi: 10.1093/nar/gkl243.

626 Lee SY, Sohn K-A, Kim JH. 2012. MicroRNA-centric measurement improves functional
627 enrichment analysis of co-expressed and differentially expressed microRNA clusters.
628 *BMC Genomics*. 13:S17. doi: 10.1186/1471-2164-13-S7-S17.

629 Leung AKL, Sharp PA. 2010. MicroRNA Functions in Stress Responses. *Mol. Cell.* 40:205–215.
630 doi: 10.1016/j.molcel.2010.09.027.

631 Liu Y, Beyer A, Aebersold R. 2016. On the Dependency of Cellular Protein Levels on mRNA
632 Abundance. *Cell*. 165:535–550. doi: 10.1016/j.cell.2016.03.014.

633 Lo Giudice C et al. 2023. UTRdb 2.0: a comprehensive, expert curated catalog of eukaryotic
634 mRNAs untranslated regions. *Nucleic Acids Res*. 51:D337–D344. doi:
635 10.1093/nar/gkac1016.

636 Lohse K, Mackintosh A, et al. 2021. The genome sequence of the large white, *Pieris brassicae*
637 (Linnaeus, 1758). *Wellcome Open Res*. 6:262. doi: 10.12688/wellcomeopenres.17274.1.

638 Lohse K, Ebdon S, et al. 2021. The genome sequence of the small white, *Pieris rapae*
639 (Linnaeus, 1758). *Wellcome Open Res*. 6:273. doi: 10.12688/wellcomeopenres.17288.1.

640 Lohse K, Hayward A, et al. 2021. The genome sequences of the male and female green-veined
641 white, *Pieris napi* (Linnaeus, 1758). *Wellcome Open Res*. 6:288. doi:
642 10.12688/wellcomeopenres.17277.1.

643 Lomsadze A, Ter-Hovhannisyan V, Chernoff YO, Borodovsky M. 2005. Gene identification in
644 novel eukaryotic genomes by self-training algorithm. *Nucleic Acids Res*. 33:6494–6506.
645 doi: 10.1093/nar/gki937.

646 Manni M, Berkeley MR, Seppey M, Simão FA, Zdobnov EM. 2021. BUSCO Update: Novel and
647 Streamlined Workflows along with Broader and Deeper Phylogenetic Coverage for
648 Scoring of Eukaryotic, Prokaryotic, and Viral Genomes. *Mol. Biol. Evol*. 38:4647–4654.
649 doi: 10.1093/molbev/msab199.

650 McGeary SE et al. 2019. The biochemical basis of microRNA targeting efficacy. *Science*.
651 366:eaav1741. doi: 10.1126/science.aav1741.

652 Mehta TK et al. 2022. Evolution of miRNA-Binding Sites and Regulatory Networks in Cichlids
653 Parsch, J, editor. *Mol. Biol. Evol*. 39:msac146. doi: 10.1093/molbev/msac146.

654 Mignone F, Gissi C, Liuni S, Pesole G. 2002. Untranslated regions of mRNAs. *Genome Biol*.
655 3:reviews0004.1. doi: 10.1186/gb-2002-3-3-reviews0004.

656 Pinzón N et al. 2017. microRNA target prediction programs predict many false positives.
657 *Genome Res*. 27:234–245. doi: 10.1101/gr.205146.116.

658 Pruisscher P, Lehmann P, Nylin S, Gotthard K, Wheat CW. 2021. Extensive transcriptomic
659 profiling of pupal diapause in a butterfly reveals a dynamic phenotype. *Mol. Ecol*. n/a.
660 doi: 10.1111/mec.16304.

661 Quinlan AR, Hall IM. 2010. BEDTools: a flexible suite of utilities for comparing genomic
662 features. *Bioinformatics*. 26:841–842. doi: 10.1093/bioinformatics/btq033.

663 Ritchie W, Flamant S, Rasko JEJ. 2009. Predicting microRNA targets and functions: traps for
664 the unwary. *Nat. Methods*. 6:397–398. doi: 10.1038/nmeth0609-397.

665 Rusin LY. 2023. Evolution of homology: From archetype towards a holistic concept of cell type.
666 *J. Morphol*. 284:e21569. doi: 10.1002/jmor.21569.

667 Sanfilippo P, Wen J, Lai EC. 2017. Landscape and evolution of tissue-specific alternative
668 polyadenylation across *Drosophila* species. *Genome Biol*. 18:229. doi: 10.1186/s13059-
669 017-1358-0.

670 Sekar V et al. 2023. Detection of transcriptome-wide microRNA–target interactions in single
671 cells with agoTRIBE. *Nat. Biotechnol*. 1–7. doi: 10.1038/s41587-023-01951-0.

672 Stanke M, Diekhans M, Baertsch R, Haussler D. 2008. Using native and syntenically mapped
673 cDNA alignments to improve de novo gene finding. *Bioinformatics*. 24:637–644. doi:
674 10.1093/bioinformatics/btn013.

675 Stanke M, Schöffmann O, Morgenstern B, Waack S. 2006. Gene prediction in eukaryotes with a
676 generalized hidden Markov model that uses hints from external sources. *BMC*
677 *Bioinformatics*. 7:62. doi: 10.1186/1471-2105-7-62.

678 Steward RA, Okamura Y, Boggs CL, Vogel H, Wheat CW. 2021. The Genome of the Margined
679 White Butterfly (*Pieris macdunnoughi*): Sex Chromosome Insights and the Power of
680 Polishing with PoolSeq Data Lavrov, D, editor. *Genome Biol. Evol.* 13:evab053. doi:
681 10.1093/gbe/evab053.

682 Stuart JM, Segal E, Koller D, Kim SK. 2003. A Gene-Coexpression Network for Global
683 Discovery of Conserved Genetic Modules. *Science*. 302:249–255. doi:
684 10.1126/science.1087447.

685 Suvorov A et al. 2022. Widespread introgression across a phylogeny of 155 *Drosophila*
686 genomes. *Curr. Biol.* 32:111-123.e5. doi: 10.1016/j.cub.2021.10.052.

687 Ter-Hovhannisyan V, Lomsadze A, Chernoff YO, Borodovsky M. 2008. Gene prediction in novel
688 fungal genomes using an ab initio algorithm with unsupervised training. *Genome Res.*
689 18:1979–1990. doi: 10.1101/gr.081612.108.

690 Trapnell C et al. 2010. Transcript assembly and quantification by RNA-Seq reveals unannotated
691 transcripts and isoform switching during cell differentiation. *Nat. Biotechnol.* 28:511–515.
692 doi: 10.1038/nbt.1621.

693 Tsang JS, Ebert MS, van Oudenaarden A. 2010. Genome-wide Dissection of MicroRNA
694 Functions and Cotargeting Networks Using Gene Set Signatures. *Mol. Cell.* 38:140–153.
695 doi: 10.1016/j.molcel.2010.03.007.

696 Wang W et al. 2019. Evolutionary and functional implications of 3' untranslated region length of
697 mRNAs by comprehensive investigation among four taxonomically diverse metazoan
698 species. *Genes Genomics*. 41:747–755. doi: 10.1007/s13258-019-00808-8.

699 Wolfe CJ, Kohane IS, Butte AJ. 2005. Systematic survey reveals general applicability of 'guilt-
700 by-association' within gene coexpression networks. *BMC Bioinformatics*. 6:227. doi:
701 10.1186/1471-2105-6-227.

702 Xu J, Wong C. 2008. A computational screen for mouse signaling pathways targeted by
703 microRNA clusters. *RNA*. 14:1276–1283. doi: 10.1261/rna.997708.

704 Ye W, Lian Q, Ye C, Wu X. 2023. A Survey on Methods for Predicting Polyadenylation Sites
705 from DNA Sequences, Bulk RNA-seq, and Single-cell RNA-seq. *Genomics Proteomics*
706 *Bioinformatics*. 21:67–83. doi: 10.1016/j.gpb.2022.09.005.

707 Zimin AV et al. 2017. Hybrid assembly of the large and highly repetitive genome of *Aegilops*
708 *tauschii*, a progenitor of bread wheat, with the MaSuRCA mega-reads algorithm.
709 *Genome Res.* 27:787–792. doi: 10.1101/gr.213405.116.

710

711